

Architectural Analysis of Human Abdominal Wall Muscles

Implications for Mechanical Function

Stephen H. M. Brown, PhD,* Samuel R. Ward, PhD,*†‡§ Mark S. Cook, PhD,¶ and Richard L. Lieber, PhD*‡

Study Design. Cadaveric analysis of human abdominal muscle architecture.

Objective. To quantify the architectural properties of rectus abdominis (RA), external oblique (EO), internal oblique (IO), and transverse abdominis (TrA), and model mechanical function in light of these new data.

Summary of Background Data. Knowledge of muscle architecture provides the structural basis for predicting muscle function. Abdominal muscles greatly affect spine loading, stability, injury prevention, and rehabilitation; however, their architectural properties are unknown.

Methods. Abdominal muscles from 11 elderly human cadavers were removed intact, separated into regions, and microdissected for quantification of physiologic cross-sectional area, fascicle length, and sarcomere length. From these data, sarcomere operating length ranges were calculated.

Results. IO had the largest physiologic cross-sectional area and RA the smallest, and would thus generate the largest and smallest isometric forces, respectively. RA had the longest fascicle length, followed by EO, and would thus be capable of generating force over the widest range of lengths. Measured sarcomere lengths, in the postmortem neutral spine posture, were significantly longer in RA and EO (3.29 ± 0.07 and $3.18 \pm 0.11 \mu\text{m}$) compared to IO and TrA

(2.61 ± 0.06 and $2.58 \pm 0.05 \mu\text{m}$) ($P < 0.0001$). Biomechanical modeling predicted that RA, EO and TrA act at optimal force-generating length in the midrange of lumbar spine flexion, where IO can generate approximately 90% of its maximum force.

Conclusion. These data provide clinically relevant insights into the ability of the abdominal wall muscles to generate force and change length throughout the lumbar spine range of motion. This will impact the understanding of potential postures in which the force-generating and spine stabilizing ability of these muscles become compromised, which can guide exercise/rehabilitation development and prescription. Future work should explore the mechanical interactions among these muscles and their relationship to spine health and function.

Key words: lumbar spine, abdominal muscles, transversus abdominis, force-length relationship, muscle, stability. **Spine 2011;36:355–362**

From the Departments of *Orthopaedic Surgery, †Radiology, and ‡Bioengineering, University of California San Diego, La Jolla, CA; §VA Medical Center, San Diego, CA; and ¶Department of Integrative Biology and Physiology, University of Minnesota, Minneapolis, MN.

Acknowledgment date: July 16, 2009. Revision date: December 8, 2009. Acceptance date: December 9, 2009.

The manuscript submitted does not contain information about medical device(s)/drug(s).

Federal funds were received in support of this work. No benefits in any form have been or will be received from a commercial party related directly or indirectly to the subject of this manuscript.

Supported by the Department of Veterans Affairs Rehabilitation Research and Development, NIH grants HD048501 and HD050837; also, supported by a Postdoctoral Fellowship from NSERC Canada (to S.H.M.B.).

IRB: Each author certifies that his or her institution has approved the protocol for this investigation and that all investigations were conducted in conformity with ethical principles of research.

Address correspondence and reprint requests to Richard L. Lieber, PhD, Department of Orthopaedic Surgery (9151), UC San Diego and VA Medical Center, 9500 Oilman Drive, Mail Code 0863, LA Jolla, CA 92093–0863; E-mail: rlieber@ucsd.edu

DOI: 10.1097/BRS.0b013e3181d12ed7

Abdominal muscles generate forces that produce movement of, and stabilize, the spinal column. They are unique morphologically: rectus abdominis (RA) is comprised of bundles of short muscle fibers arranged in-series to create one longer muscle; external oblique (EO), internal oblique (IO), and transverse abdominis (TrA) are tightly bound layered muscular sheets with fibers running at oblique angles to one another. As a composite, these muscles function together to pressurize the abdominal cavity and transfer forces around the torso. However, very little is understood about the structural design of these muscles, in particular the fiber arrangement in-series and in-parallel throughout the muscles. This design, known as muscle architecture, is imperative to the understanding of the function of these muscles. Therefore, this study was undertaken to examine the architectural properties of the 4 abdominal muscles.

Muscle architectural design dictates, in large part, a muscle's functional capacity.¹ Physiologic cross-sectional area (PCSA) represents the number of force-generating sarcomeres arranged in-parallel and predicts its maximum isometric force generating capability.² The number of sarcomeres arranged in-series through the muscle, represented by its optimal fascicle length for maximum force generation, determines the absolute length range, as well as the maximum velocity, over which a muscle can actively generate force.¹ A longer fibered

muscle can produce force over a greater range of lengths, as a greater number of sarcomeres will act to effectively produce this overall length change. This also has direct implications for the velocities at which a muscle can produce force, because again, in muscles with long fibers each sarcomere will have a lower relative velocity compared to a muscle with short fibers.

PCSA of the abdominal muscles has been estimated using a number of imaging methods (computed tomography, MRI, ultrasound),³⁻⁵ but these estimates are suspect since no single image can capture all fibers across these uniquely shaped muscles, and assumptions must be made to correct for muscle fiber lines of action oriented relative to image planes. The only way to reliably define muscle force generating properties is to microdissect individual muscles and thus provide reliable measures of the arrangement of contractile material in the muscle.

Biomechanical estimates of spine loading and stability rely heavily on knowledge of muscular force and stiffness generation. The abdominal muscles, in particular, have been widely studied in terms of their role in spinal loading and stability.⁶⁻¹¹ Unfortunately, even the most sophisticated biomechanical spine models still rely heavily on assumptions regarding abdominal muscle architecture, specifically the force-length and force-velocity properties of these muscles. Architectural analysis provides information regarding muscle sarcomere arrangement that, in large part, determines a muscle's maximum force capability, as well as length- and velocity-dependent characteristics. Therefore, the purpose of this study was to define the architectural properties of the human abdominal muscles.

MATERIALS AND METHODS

Eleven formaldehyde-fixed cadaveric donors were studied (5 male, mean \pm standard deviation age = 71.8 ± 17.9 years, height = 174.8 ± 6.6 cm, mass = 67.8 ± 9.4 kg; 6 female, age = 82.7 ± 14.5 years, height = 165.6 ± 3.7 cm, mass = 63.1 ± 11.8 kg). All donors died of natural (nontraumatic) causes. None of the donors had any gross spinal-related injury or pathology, and abdominal wall muscles were inspected in all cadavers to ensure that no noticeable defect or pathology existed.

It was important that the muscles were fixed while attached to the skeleton, before dissection, to preserve them at their neutral spine posture length. Each of the 4 abdominal muscles was dissected from one side of the body and removed intact. Muscles were then divided regionally as follows: RA along each of its transverse tendinous intersections (8 donors had 3 such intersections and therefore 4 regions, 2 donors 2 intersections and therefore 3 regions, and 1 donor 4 intersections and therefore 5 regions); EO, IO, and TrA were each divided into 3 regions, determined to maintain approximately homogenous fascicle lengths within each region (Figure 1).

Tendon, connective tissues and adipose were removed, and each muscle region was gently blotted dry and weighed (resolution 0.01 g) to determine mass, and the length of the longest fascicles within each region was measured (Figure 2) with a

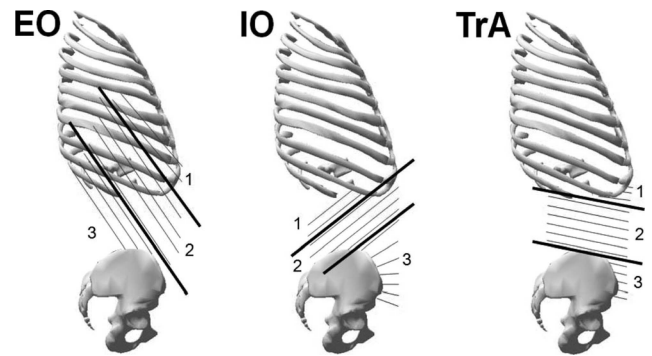


Figure 1. Schematic representation of the regional divisions of EO, IO, and TrA used for the architectural analysis. Thick black lines represent the approximate regional divisions. Note that the schematic is intended only to display the regionalization, and not necessarily to represent PCSA or fascicle length. The purpose of dividing the muscles into regions was to determine whether there was specialization of muscle architecture within muscles.

digital caliper (resolution 0.01 mm). PCSA was calculated using the following equation¹²:

$$PCSA(\text{cm}^2) = \frac{M(\text{g}) * \cos(\theta)}{\rho \left(\frac{\text{g}}{\text{cm}^3} \right) * L_{fn}(\text{cm})} \quad (1)$$

where, M = muscle mass, L_{fn} = normalized fascicle length (described below), θ = pennation angle (0° for all abdominal muscles), and ρ = density of muscle fixed in 37% formaldehyde (1.112 g/cm^3).¹³

A minimum of 3 small fiber bundles (composed of ~ 50 fibers) were dissected free from each muscle region, and sarcomere length was measured using laser diffraction at multiple locations (at least 3, randomly selected) along each bundle.¹⁴ The number

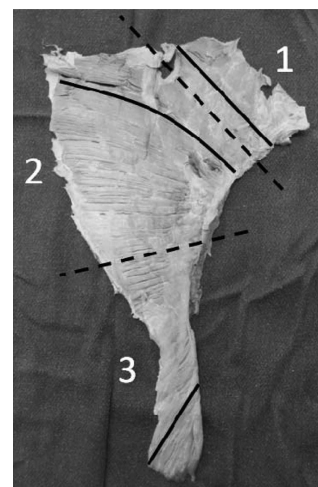


Figure 2. Example of IO fascicle measurements. Dashed lines represent division of muscle into 3 regions. Solid lines represent fascicle lengths measured with digital caliper (note: fascicle in region 2 would be straightened to enable measurement). Each region was then separated and weighed. Normalized fascicle lengths were determined from equation 2 after sarcomere length measurement. Normalized fascicle lengths and masses for each region were used to calculate PCSA.

of sarcomeres arranged in-series within each muscle region was calculated by dividing measured fascicle length (converted to μm) by average measured sarcomere length. Normalized fascicle lengths were calculated using the equation:

$$Lf_n(\text{cm}) = Lf_m(\text{cm}) * \left(\frac{Ls_o(\mu\text{m})}{Ls_m(\mu\text{m})} \right) \quad (2)$$

where, Lf_m = measured fascicle length, Ls_m = measured sarcomere length, Ls_o = optimal sarcomere length for human muscle ($2.70 \mu\text{m}$, the midplateau of the relationship defined by Walker and Schrodt¹⁵).

Whole muscle architectural properties were determined as follows for each donor cadaver: RA (where regions act in-series [are connected end-to-end, and therefore share equal force in each region]) PCSA was calculated as the largest measured regional PCSA; RA fascicle length, in-series sarcomere number, and normalized length were summed for all regions; RA sarcomere length was averaged across all regions; EO, IO, and TrA (where regions act in-parallel [are connected side-to-side, and therefore summate their independent forces]) PCSA was summed across all regions; EO, IO, and TrA fascicle length, sarcomere length, in-series sarcomere number, and normalized length were calculated as weighted averages (weighted to regional PCSAs) across all regions.

For modeling purposes, skeletal abdominal muscle origins and insertions were taken from the models of McGill⁴ and Cholewicki and McGill.¹⁶ Superior muscle attachments were rotated with the skeleton through average ranges of lumbar motion about each of the functional spine axes (flexion/extension, lateral bend, axial twist), while pelvic-level attachments remained fixed. This simulates the changing length of each muscle as the lumbar spine moves through its range of motion. The modeled ranges of motion were: flexion, 52° ¹⁷; extension, 16° ¹⁷; lateral bend, 29° each ipsilateral and contralateral¹⁸; axial twist, 9° each ipsilateral and contralateral.¹⁸ Relative muscle length change was calculated, and from this, sarcomere length change was calculated across the range of motion (assuming that the cadaveric-measured sarcomere lengths correspond to the neutral spine posture). McGill⁴ modeled IO and EO muscles as consisting of 2 separate lines of action (representing anterior and lateral fibers, respectively), with corresponding separate skeletal attachments. All 4 of these lines of action were modeled here, but within EO and IO only the line of action that resulted in the largest relative length change (and thus largest sarcomere length range) is reported. Sarcomere length ranges are then plotted with respect to the well-known sarcomere force-length relationship, originally defined for frog muscle by Gordon *et al*,¹⁹ and here adjusted for human muscle actin filament lengths.

Whole-muscle architectural variables (PCSA, fascicle length, normalized fascicle length, sarcomere length) were first correlated with possible covariates age and body mass index (BMI). Depending on whether statistically significant correlations were determined, architectural variables were compared by either 2-way mixed model analysis of variance or analysis of covariance (muscle as a repeated measure, and gender as the independent factor). Tukey's HSD *post hoc* test

was used when significant effects were revealed by analysis of variance. Statistical significance was set at $P < 0.05$.

RESULTS

Muscle PCSA correlated significantly with both age ($r = -0.33, P = 0.03$) and BMI ($r = 0.39, P = 0.008$). Architectural characteristics of the muscles and muscle regions are shown in Table 1. Muscle PCSA, indicating maximal force generating capacity, and normalized length, indicating excursion potential, are also plotted in Figure 3. While a range of excursion and force-generating potential exists, at the extremes it is clear that IO is designed for the greatest force production (PCSA = $8.6 \pm 0.8 \text{ cm}^2$), but over the smallest range of lengths (normalized fascicle length = $7.8 \pm 0.4 \text{ cm}$), whereas RA is designed to produce large length changes (normalized fascicle length = $26.7 = 1.6 \text{ cm}$) while generating the smallest amount of force (PCSA = $3.3 \pm 0.5 \text{ cm}^2$). No gender effects were found for any tested variable.

In the postmortem spine posture, sarcomere lengths of RA ($3.29 \pm 0.07 \mu\text{m}$) and EO ($3.18 \pm 0.11 \mu\text{m}$) were statistically greater than IO ($2.61 \pm 0.06 \mu\text{m}$) and TrA (2.58 ± 0.05) ($P < 0.0001$).

The largest sarcomere operating range was predicted for RA in flexion/extension, EO, and IO in lateral bend, and TrA in axial twist (Figure 4). All muscles act across the plateau region of the force-length curve when lengthened about a minimum of 1 of the 3 axes of rotation. Between 25° and 28° of lumbar flexion, modeled sarcomere lengths of RA, EO, and TrA are on the plateau of the force-length curve (where they can generate maximum isometric force), while sarcomeres within the lateral and anterior fibers of IO act at approximately 2.95 and $2.32 \mu\text{m}$, respectively (at which point the muscle could still generate approximately 90% of its maximum force) (Figure 5). RA, lateral fibers of EO, and postero- F5 lateral IO fibers act well down the descending limb of the force-length curve (where their active force generating capability can be severely compromised) in contralateral bend, as do RA and EO in full extension and posterolateral fibers of IO in full flexion (Figure 4). TrA undergoes the smallest length changes through lumbar ROM, and therefore is maintained near the plateau of the force-length relationship (Figure 4).

DISCUSSION

This is the first to study define the detailed architecture of the abdominal muscles, and interpret their function based on architectural parameters. In particular, important information regarding force generating potential, serial sarcomere number and lengths (indicating absolute muscle lengths and velocities over which a muscle can generate force) are reported. These properties define the structural basis for predicting muscle function, and based on estimated sarcomere length operating ranges, describe the ability of muscles to generate active force and stiffness through the lumbar spine range of motion. Furthermore, these data serve as vital inputs to biomechanical models that assess spine loads and stability.

A graphical representation of the functional capabilities of the abdominal muscles is displayed in Figure 3. PCSA is directly

TABLE 1. Architectural Properties of Human Abdominal Wall Muscles

Muscle (Region)	Mass (g)	Fascicle Length (cm)	PCSA (cm ²)	Sarcomere Length (μm)	Sarcomere Number	Normalized Fascicle Length (cm)
RA (whole)	80.8 ± 15.0	34.2 ± 1.9*	3.3 ± 0.5*	3.29 ± 0.07*	98,747 ± 5795	26.7 ± 1.6*
RA1	12.4 ± 2.2	6.7 ± 0.6	2.1 ± 0.3	3.22 ± 0.13	21,152 ± 1771	5.7 ± 0.5
RA2	15.6 ± 2.7	6.6 ± 0.4	2.6 ± 0.5	3.24 ± 0.09	20,261 ± 1117	5.5 ± 0.3
RA3	25.0 ± 7.1	10.6 ± 1.6	2.5 ± 0.4	3.30 ± 0.10	31,816 ± 4475	8.6 ± 1.2
RA4	27.8 ± 3.7	12.1 ± 1.0	2.7 ± 0.5	3.36 ± 0.15	31,885 ± 3412	9.7 ± 0.9
RA5 (n = 1)	69.2 ± 0.0	13.2 ± 0.0	6.4	3.67 ± 0.0	36,038 ± 0	9.7 ± 0.0
EO (whole)	104.6 ± 11.8	17.0 ± 0.9†	6.6 ± 0.9†	3.18 ± 0.11*	53,893 ± 3604	14.6 ± 1.0†
EO1	16.1 ± 2.5	11.2 ± 1.0	1.6 ± 0.2	3.25 ± 0.07	34,812 ± 2313	9.4 ± 0.6
EO2	67.8 ± 9.4	19.9 ± 0.9	3.7 ± 0.6	3.22 ± 0.12	62,325 ± 3264	16.8 ± 0.9
EO3	20.7 ± 2.1	15.9 ± 0.8	1.5 ± 0.2	3.01 ± 0.12	50,626 ± 4050	13.7 ± 1.1
IO (whole)	74.4 ± 6.8	7.9 ± 0.5‡	8.6 ± 0.8‡	2.61 ± 0.06†	28,715 ± 1619	7.8 ± 0.4‡
IO1	15.1 ± 1.7	7.4 ± 0.3	2.0 ± 0.2	2.78 ± 0.10	26,922 ± 1697	7.3 ± 0.5
IO2	39.6 ± 4.1	11.2 ± 0.7	3.2 ± 0.3	2.63 ± 0.08	42,662 ± 2777	11.5 ± 0.7
IO3	19.7 ± 2.1	4.9 ± 0.5	3.5 ± 0.4	2.54 ± 0.08	19,387 ± 1785	5.2 ± 0.5
TrA (whole)	50.6 ± 5.1	9.5 ± 0.4‡	4.7 ± 0.6*†	2.58 ± 0.05†	36,051 ± 1601	9.7 ± 0.4‡
TrA1	11.2 ± 2.2	7.6 ± 0.3	1.5 ± 0.3	2.57 ± 0.10	27,015 ± 1470	7.3 ± 0.4
TrA2	28.5 ± 2.7	13.8 ± 0.5	1.8 ± 0.2	2.61 ± 0.05	54,916 ± 2257	14.8 ± 0.6
TrA3	11.9 ± 1.8	6.6 ± 0.5	1.6 ± 0.4	2.47 ± 0.06	26,878 ± 2021	7.3 ± 0.5

Statistical tests were conducted on fascicle length, PCSA, sarcomere length and normalized fascicle length. Different symbols (*, †, ‡) indicate statistically significant differences between muscles. Data represented as mean ± standard error of the mean (SEM) (n = 11).

PCSA indicates physiologic cross-sectional area; RA, rectus abdominis; EO, external oblique; IO, internal oblique; TrA, transverse abdominis.

proportional to maximum force production,² while normalized muscle fascicle length is proportional to maximal excursion.²⁰ Muscles composed of a high number of sarcomeres arranged in-parallel can generate large forces. Muscles with a high number of sarcomeres arranged in-series can generate force over

large absolute length ranges, as each sarcomere can accommodate a specific absolute length change based on its force-length relationship. Thus, a greater number of sarcomeres changing length and acting in-series will sum to create a greater overall change in muscle length. Long fibered muscles can thus also generate force at higher absolute velocities, as again, each sarcomere undergoes a smaller absolute length change with time. Therefore, based on architectural properties, IO has the potential to generate the greatest isometric force, but over a small length range. RA, at the other extreme, comprised of shorter fibers in-series across 3 to 5 bundled regions, can generate relatively little isometric force, but accommodates the large length changes that can occur during spine flexion/extension. EO can also generate active force across a fairly wide range of lengths and velocities, and primarily accommodate these changes during lateral bend. TrA appears to play an intermediate role, with a modest PCSA and shorter normalized length.

The predicted sarcomere operating ranges of the abdominal muscles, over full range of motion about each of the 3 anatomic spine axes, are displayed in Figure 4. The widest predicted operating ranges occur for the lateral fibers of both EO and IO during lateral bend, as these muscles undergo large relative length changes through the range of ipsilateral to contralateral bend. This demonstrates that these muscle regions have a compromised ability to generate active force when the spine is laterally bent to the contralateral side. It is important to note that, at the same time, the more anterior

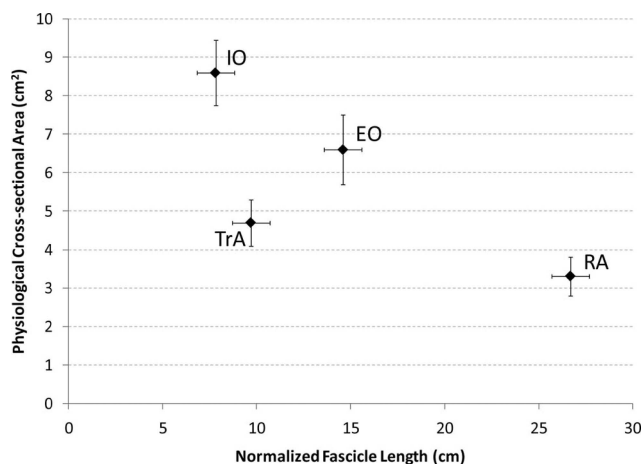


Figure 3. Scatter plot of PCSA and normalized fascicle lengths of the abdominal muscles. RA fascicle length represents the total in-series length across all regions. Large PCSA indicates large isometric force generating ability, and a long normalized fascicle length indicates the ability to generate force across a wide range of lengths. Data are plotted as mean ± SEM.

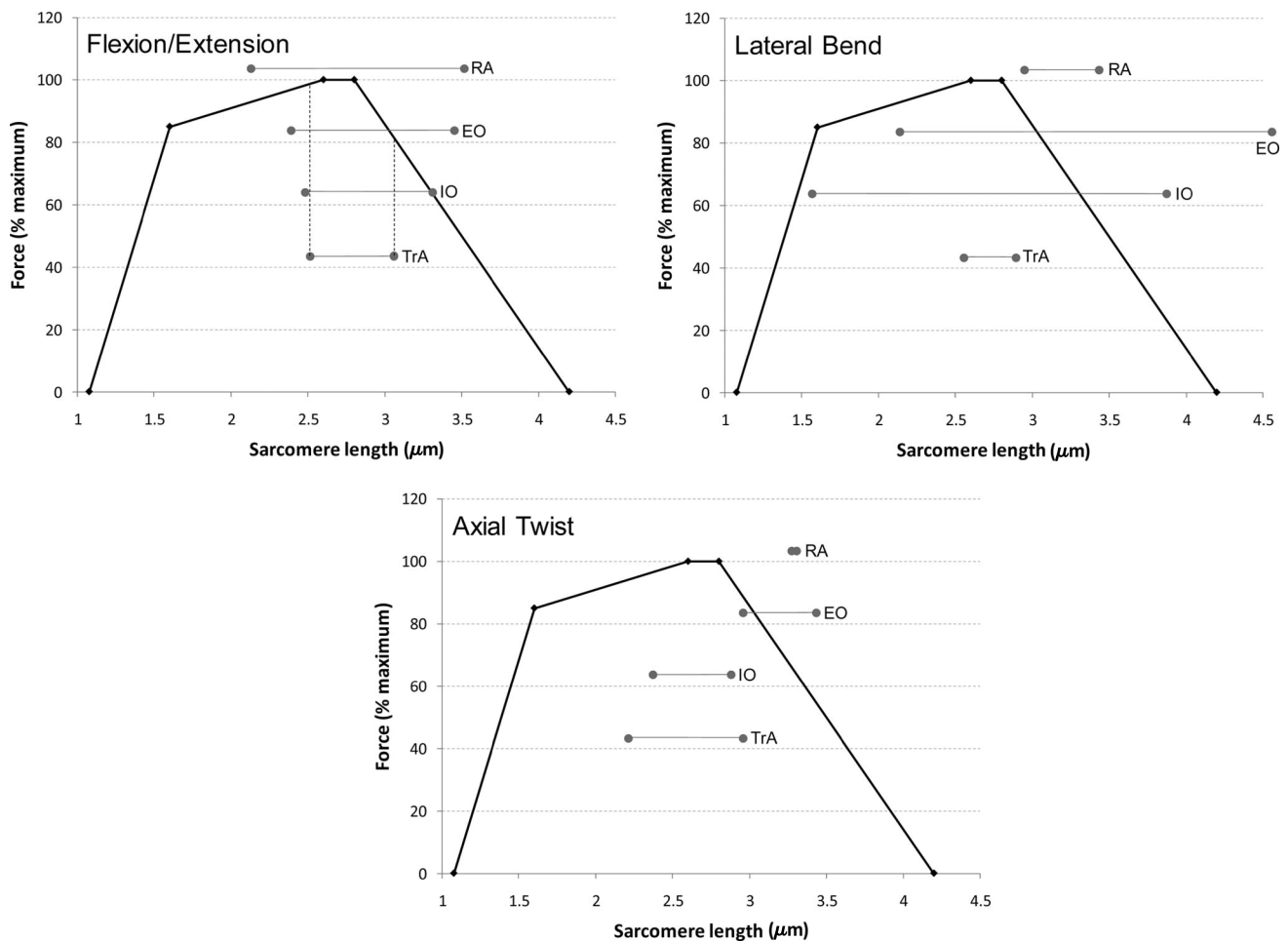


Figure 4. Predicted sarcomere length operating ranges (represented by horizontal lines for each muscle) across the lumbar range of motion of each spine anatomic axis. An interpretive example is shown for TrA in flexion/extension: the dashed lines are projected vertically onto the force-length curve to demonstrate the operating range of the muscle. Operating ranges represent the maximum for fibers of any region within each muscle. Flexion/extension: RA and EO are long in extension, TrA and lateral fibers of IO are long in flexion; Lateral Bend: RA, lateral fibers of both EO and IO are long in contralateral bend, TrA is long in ipsilateral bend; Axial Twist: RA and lateral fibers of EO are long in ipsilateral twist, TrA and lateral fibers of IO are long in contralateral twist. The force-length relationship is estimated for human muscle assuming myosin and actin filament lengths of 1.6 and 1.3 μm , respectively.

fibers of EO and IO act near the plateau of the force-length relationship during contralateral bend. Additionally, RA and EO appear to be compromised in their force generating capability during extreme spine extension, while posterolateral fibers of IO become compromised in full flexion (Figures 4 and 5). TrA, on the other hand, due to its modest length changes throughout the lumbar spine range of motion, acts almost exclusively around the plateau of its force-length relationship, where its force-generating ability is near maximum. It should be noted that the operating ranges reported here are based on a model of muscle lengthening/shortening along straight lines between moving skeletal attachments, and do not account for potential folding or bunching of the muscles that might occur in flexion (primarily RA) and lateral bend (primarily EO, IO, and TrA). Further, these estimates assume a purely passive ROM and do not account for further shortening of the muscles that could occur during contraction due to in-series connective tissue compliance. Future work must

quantify these relative compliances, and well as the interaction between the tightly bound adjacently-layered muscles, to fully elucidate the *in vivo* lengthening and shortening contraction dynamics.

Measured sarcomere length, in the neutral spine postmortem state, was above optimal for RA and EO (3.29 and 3.18 μm , respectively), and slightly below optimal for IO and TrA (2.61 and 2.58 μm , respectively). Based on their known skeletal attachments, fibers of RA and EO will shorten with spine flexion, while a bulk of IO and TrA fibers lengthen with spine flexion. Modeling the length changes of these muscles during flexion/extension predicts that RA, EO, TrA act together on the plateau of the force-length relation from 25° to 28° of spine flexion (approximately 50% of the average ROM; Figure 5). The lateral and anterior fibers of IO, that lengthen and shorten during flexion, respectively, would have sarcomere lengths of approximately 2.95 and 2.32 μm (still capable of producing approximately 90% of maximum isometric force)

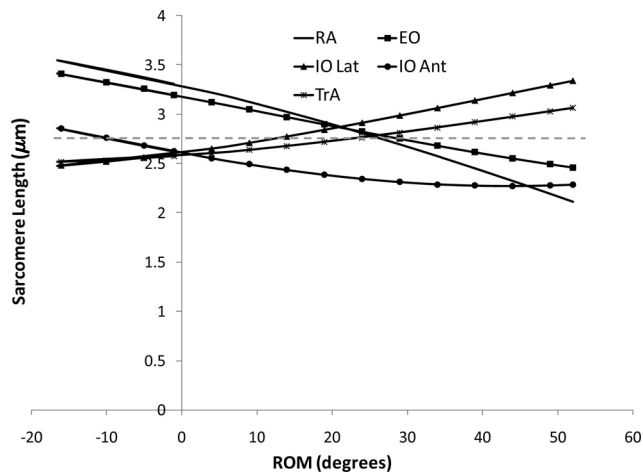


Figure 5. Sarcomere length changes for RA, EO, TrA, and anterior (ant) and lateral (lat) IO fibers across the lumbar spine flexion/extension range of motion. Positive ROM values indicate flexion while negative values represent extension. The horizontal dashed line represents the approximate optimal sarcomere length for human muscle ($2.7 \mu\text{m}$).

at the same spine angles. Thus, based on this model, IO does not act at optimal length at the same spine posture as the other 3 abdominal muscles, and further, fibers within anterior *versus* lateral regions of IO may achieve optimal length at different respective spine postures. However, since IO can still generate approximately 90% of its maximum force when the other 3 muscles are at optimum it appears that the abdominal muscles, as a whole, are optimized to generate peak force in the midrange of lumbar spine flexion. That the abdominal muscles act across the plateau of the force-length relation differs from other reported muscle groups such as the wrist flexors²¹ and multifidus,²² both of which act primarily on the ascending limb of the curve, or the wrist extensors which operate primarily on the descending limb.²⁰

The majority of the estimates of physiologic cross-sectional area (PCSA) of the abdominal muscles come from imaging methods (CT, MRI, ultrasound). These studies consistently estimate larger PCSAs compared to those reported here for the RA (Reid and Costigan,²³ McGill *et al*,³ and Marras *et al*,⁵ ranging between 6 and 10.5 cm^2), IO and EO (McGill⁴ approximately 16 cm^2 and 19 cm^2 for the EO and IO, respectively; Stokes and Gardner-Morse²⁴ approximately 16 cm^2 and 13 cm^2 for the EO and IO, respectively). Delp *et al*,²⁵ examining 5 elderly cadavers, measured an average PCSA of the RA of 2.6 cm^2 , comparable to the value of 3.3 cm^2 measured here. The discrepancies between the cadaveric and imaged estimates of PCSA may suggest an age-related muscular atrophy since the average age range in the imaging studies was 25 to 53 years compared to the average age of 77.7 ± 16.3 years in this report. However, the main problem with using imaging methods to estimate PCSA is that areas are measured in one of the cardinal anatomic planes. Since PCSA is supposed to estimate the total number of sarcomeres acting in parallel, or the total cross-sectional area of contracting muscle, this type of imaging is prone to error since it is dif-

icult to include an estimate of fibers that are not in any single imaged plane (which would happen, for example, with the IO, since no single slice can contain all the fibers), nor does it necessarily include the appropriate correction for muscle fibers at an angle relative to the imaging plane. To date, no study has directly compared these methods for PCSA estimation, although the use of dissection-derived PCSA values has been validated against direct measurement of muscle force.² Future studies are required to elucidate the differences between PCSA values derived using different methodologies. In the meantime, consideration of architectural data from multiple sources and methodologies is warranted to develop a representative and reliable data set.

With regards to sarcomere lengths, RA is the only human muscle that has been examined.²⁵ Mean sarcomere lengths measured in the neutral spine postmortem position was $2.83 \pm 0.13 \mu\text{m}$, well below the $3.29 \pm 0.07 \mu\text{m}$ that we measured in the current study. The discrepancy is most likely due to the fact that, in the Delp *et al*²⁵ study, muscles were formalin-fixed after removal from the skeleton, which allows sarcomeres to shorten during fixation.

There are several limitations that must be stated with regard to the data reported here. First, it is well established that intervertebral discs absorb fluid and swell under decreased external loading,²⁶ causing an overall spinal column lengthening.²⁷ Spine length over the combined lumbar/thoracic levels can vary in the range of 1.8 cm over the course of a day,²⁸ with 54% of height loss occurring in the first hour after waking.²⁷ In the postmortem state, discs will be highly hydrated, causing a lengthening of the muscles crossing these joints that may be more representative of the *in vivo* muscle lengths immediately after awaking. Alternatively, in the postmortem state, the abdomen is not pressurized, which in the supine position may permit relative shortening of the abdominal muscles as they are allowed to relax into the abdominal cavity. It is not clear what effect these 2 factors have (if any) on measured muscle fascicle and sarcomere lengths, but they should be considered in the interpretation of sarcomere length operating ranges. Note that sarcomere number and normalized fiber length calculations are independent of the absolute length at which measurements are taken, and can be considered faithful. Second, no correction was made for series tendon compliance when calculating operating range. Tendon compliance can have a significant impact on muscle sarcomere length ranges depending on the length of the tendon in series with the fibers²⁹⁻³¹ and the material properties of the tendon itself.^{29,32} In particular, a high tendon length:muscle length ratio can greatly affect the force-length³¹ and even the dynamic properties³³ of the muscle. Such an effect could vary greatly for each abdominal muscle, or even within different regions of the muscles. For example, RA, and fibers of EO and IO that span from the pelvis to rib cage, have very little tendinous material; however, fibers of EO, IO, and TrA that terminate across the rectus sheath and/or lumbar fascia may have large in-series compliances. Future work will need to examine the relative tendon length-muscle fiber length ratios for the various regions of these muscles, to determine potential physiologic impact. Third, as mentioned above, it is possible that, due to the advanced age of the cadaveric specimens,

the PCSA values are unrepresentative of those found in normal adults. Previous comparisons of young and elderly adult subjects have revealed PCSA differences often greater than 50%,³⁴ and we found a statistically significant negative correlation ($r = -0.33$) between PCSA and the range of ages that we studied. Thus, the values reported here may underestimate those found in healthy adults. It should be noted that the relative PCSA ratios will probably not be affected by abdominal wall muscle atrophy.³⁵ Parallel comparisons of PCSA using several methods across a wide age range will resolve this issue. Finally, gender comparisons were made on a relatively small sample size (5 male and 6 female) of elderly individuals. Although no statistical differences between the genders were observed, it is possible that with a larger, and/or younger, sample statistical differences would emerge.

Finally, note that this study considered abdominal muscles in isolation. However, in light of the unique layered morphology of the abdominal muscle wall, future work is required to explore the magnitude and significance (if any) of the interaction among muscle layers.

Muscle contraction (shortening and lengthening), force generation and force transfer could be significantly impacted by the mechanical interaction among muscle layers.³⁵⁻³⁷ Further, abdominal obesity may affect the resting length and contractile function of the abdominal muscles, and future work will need to address any physiologic significance stemming from this effect. Thus, while the architectural data reported here provide much needed understanding of the underlying structure of the abdominal muscles, complete elucidation of their mechanical function will require study and consideration of these muscles under more realistic *in vivo* conditions.

➤ Key Points

- Abdominal wall muscles were dissected from 11 elderly cadavers, and measured for architectural parameters such as physiologic cross-sectional area and fascicle length, which were used to predict force-length properties.
- IO has the largest isometric force generating potential, whereas RA can generate force across the greatest range of lengths.
- In the neutral spine posture, sarcomeres of RA and EO (3.29 and 3.18 μm , respectively) were longer than optimal length for maximum force generation, while those of IO and TrA (2.61 and 2.58 μm , respectively) were slightly below optimal length.
- Biomechanical modeling predicts that RA, EO, and TrA act at optimal length for maximum force generation in the midrange of lumbar spine flexion, where IO can generate approximately 90% of its maximum isometric force.
- Caution should be used regarding the absolute values for muscle physiologic cross-sectional area and fascicle length, as the means reported in the current study represent an elderly population.

References

1. Lieber RL, Friden J. Functional and clinical significance of skeletal muscle architecture. *Muscle Nerve* 2000;23:1647-66.
2. Powell PL, Roy RR, Kanim P, et al. Predictability of skeletal muscle tension from architectural determinations in guinea pig hindlimbs. *J Appl Physiol* 1984;57:1715-21.
3. McGill SM, Patt N, Norman RW. Measurement of the trunk musculature of active males using CT scan radiography: implications for force and moment generating capacity about the L4/L5 joint. *J Biomech* 1988;21:329-41.
4. McGill SM. A revised anatomical model of the abdominal musculature for torso flexion efforts. *J Biomech* 1996;29:973-7.
5. Marras WS, Jorgensen MJ, Granata KP, et al. Female and male trunk geometry: size and prediction of the spine loading trunk muscles derived from MRI. *Clin Biomech* 2001;16:38-46.
6. Axler CT, McGill SM. Low back loads over a variety of abdominal exercises: searching for the safest abdominal challenge. *Med Sci Sports Exerc* 1997;29: 804-11.
7. Gardner-Morse MG, Stokes IAF. The effects of abdominal muscle coactivation on lumbar spine stability. *Spine* 1998;23:86-91.
8. de Looze MP, Groen H, Horemans H, et al. Abdominal muscles contribute in a minor way to peak spinal compression in lifting. *J Biomech* 1999;32: 655-62.
9. Granata KP, Orishimo KF. Response of trunk muscle coactivation to changes in spinal stability. *J Biomech* 2001;34:1117-23.
10. Brown SHM, Vera-Garcia FJ, McGill SM. Effects of abdominal muscle co-activation on the externally preloaded trunk: variations in motor control and its effect on spine stability. *Spine* 2006;31: E387-93.
11. El Ouaaid Z, Arjmand N, Shirazi-Adl A, et al. A novel approach to evaluate abdominal coactivities for optimal spinal stability and compression force in lifting. *Comput Meth Biomech Biomed Eng* 2009;12:735-45.
12. Sacks RD, Roy RR. Architecture of the hind limb muscles of cats: functional significance. *J Morphol* 1982;173:185-95.
13. Ward SR, Lieber RL. Density and hydration of fresh and fixed human skeletal muscle. *J Biomech* 2005;38:2317-20.
14. Lieber RL, Fazeli BM, Botte MJ. Architecture of selected wrist flexor and extensor muscles. *J Hand Surg (Am)* 1990;15:244-50.
15. Walker SM, Schrodt GR. I segment lengths and thin filament periods of skeletal muscle fibers of the rhesus monkey and the human. *Anat Rec* 1974; 178:63-82.
16. Cholewicki J, McGill SM. Mechanical stability of the in vivo lumbar spine: implications for injury and chronic low back pain. *Clin Biomech* 1996;11: 1-15.
17. Pearce M, Portek I, Shepherd J. 3-dimensional x-ray analysis of normal movement in the lumbar spine. *Spine* 1984;9:294-7.
18. White AA, Panjabi MM. *Clinical Biomechanics of the Spine*. 2nd ed. Philadelphia, PA: J.B. Lippincott Company; 1990.
19. Gordon AM, Huxley AF, Julian FJ. The variation in isometric tension with sarcomere length in vertebrate muscle fibres. *J Physiol* 1966;184:170-92.
20. Bodine SC, Roy RR, Meadows DA, et al. Architectural, histochemical, and contractile characteristics of a unique biarticular muscle: the cat semitendinosus. *J Neurophysiol* 1982;48:192-201.
21. Loren GJ, Shoemaker SD, Burkholder TJ, et al. Human wrist motors: biomechanical design and application to tendon transfers. *J Biomech* 1996;29: 331-42.
22. Ward SR, Kim CW, Eng CM, et al. Architectural analysis and intraoperative measurements demonstrate the unique design of the multifidus muscle for lumbar spine stability. *J Bone J Surg* 2009;91:176-85.
23. Reid JG, Costigan PA. Geometry of adult rectus abdominis and erector spinae muscles. *J Orthop Sports Phys Ther* 1985;6:278-80.
24. Stokes IAF, Gardner-Morse M. Quantitative anatomy of the lumbar musculature. *J Biomech* 1999;32:311-6.
25. Delp SL, Suryanarayanan S, Murray WM, et al. Architecture of the rectus abdominis, quadratus lumborum, and erector spinae. *J Biomech* 2001;34: 371-5.
26. Urban JPG, McMullin JF. Swelling pressure of the lumbar intervertebral discs: influence of age, spinal level, composition, and degeneration. *Spine* 1988;13:179-87.

27. Tyrell AR, Reilly T, Troup JD. Circadian variation in stature and the effects of spinal loading. *Spine* 1985;10:161–4.
28. Adams MA, Dolan P, Hutton WC. Diurnal variations in the stresses on the lumbar spine. *Spine* 1987;12:130–7.
29. Zajac FE. Muscle and tendon: properties, models, scaling, and application to biomechanics and motor control. *Crit Rev Biomed Eng* 1989;17:359–411.
30. Lieber RL, Leonard ME, Brown CG, et al. Frog semitendinosus tendon load-strain and stress-strain properties during passive loading. *Am J Physiol* 1991;261:C86–92.
31. Lieber RL, Brown CG, Trestik CL. Model of muscle-tendon interaction during frog semitendinosus fixed-end contractions. *J Biomech* 1992;25: 421–8.
32. Loren GJ, Lieber RL. Tendon biomechanical properties enhance human wrist muscle specialization. *J Biomech* 1995;28:791–9.
33. Griffiths RI. Shortening of muscle fibres during stretch of the active cat medial gastrocnemius muscle: the role of tendon compliance. *J Physiol* 1991; 436:219–36.
34. Cutts A, Seedhom BB. Validity of cadaveric data for muscle physiological cross-sectional area ratios: a comparative study of cadaveric and in-vivo data in human thigh muscles. *Clin Biomech* 1993;8:156–62.
35. Huijing PA. Muscle as a collagen fiber reinforced composite: a review of force transmission in muscle and whole limb. *J Biomech* 1999;32:329–45.
36. Maas H, Yucesoy CA, Baan GC, et al. Implications of muscle relative position as a co-determinant of isometric muscle force: a review and some experimental results. *J Mech Med Biol* 2003;3:145–68.
37. Brown SHM, McGill SM. Transmission of muscularly generated force and stiffness between layers of the rat abdominal wall. *Spine* 2009;34:E70–5.